

Review

Sorafenib-Based Drug Delivery Systems: Applications and Perspectives

Lingyun Wang ^{1,*} , Meihuan Chen ¹, Xueguang Ran ², Hao Tang ¹ and Derong Cao ¹ 

¹ Key Laboratory of Functional Molecular Engineering of Guangdong Province, School of Chemistry and Chemical Engineering, South China University of Technology, 381 Wushan Road, Guangzhou 510641, China; jasmine80420@163.com (M.C.); haotang@scut.edu.cn (H.T.); drcao@scut.edu.cn (D.C.)

² Institute of Animal Science, Guangdong Academy of Agricultural Sciences, Ministry of Agriculture Key Laboratory of Animal Nutrition and Feed Science in South China, State Key Laboratory of Livestock and Poultry Breeding, Guangzhou 510641, China; rxg59@aliyun.com

* Correspondence: lingyun@scut.edu.cn

Abstract: As a Food and Drug Administration (FDA)-approved molecular-targeted chemotherapeutic drug, sorafenib (SF) can inhibit angiogenesis and tumor cell proliferation, leading to improved patient overall survival of hepatocellular carcinoma (HCC). In addition, SF is an oral multikinase inhibitor as a single-agent therapy in renal cell carcinoma. However, the poor aqueous solubility, low bioavailability, unfavorable pharmacokinetic properties and undesirable side effects (anorexia, gastrointestinal bleeding, and severe skin toxicity, etc.) seriously limit its clinical application. To overcome these drawbacks, the entrapment of SF into nanocarriers by nanoformulations is an effective strategy, which delivers SF in a target tumor with decreased adverse effects and improved treatment efficacy. In this review, significant advances and design strategies of SF nanodelivery systems from 2012 to 2023 are summarized. The review is organized by type of carriers including natural biomacromolecule (lipid, chitosan, cyclodextrin, etc.); synthetic polymer (poly(lactic-co-glycolic acid), polyethyleneimine, brush copolymer, etc.); mesoporous silica; gold nanoparticles; and others. Co-delivery of SF and other active agents (glypican-3, hyaluronic acid, apolipoprotein peptide, folate, and superparamagnetic iron oxide nanoparticles) for targeted SF nanosystems and synergistic drug combinations are also highlighted. All these studies showed promising results for targeted treatment of HCC and other cancers by SF-based nanomedicines. The outlook, challenges and future opportunities for the development of SF-based drug delivery are presented.

Keywords: sorafenib; multi-kinase inhibitor; nanodelivery systems; hepatocellular carcinoma (HCC); nano-sized carriers; tumor treatment



Citation: Wang, L.; Chen, M.; Ran, X.; Tang, H.; Cao, D. Sorafenib-Based Drug Delivery Systems: Applications and Perspectives. *Polymers* **2023**, *15*, 2638. <https://doi.org/10.3390/polym15122638>

Academic Editor: Ángel V. Delgado

Received: 27 April 2023

Revised: 2 June 2023

Accepted: 7 June 2023

Published: 9 June 2023



Copyright: © 2023 by the authors. Licensee MDPI, Basel, Switzerland. This article is an open access article distributed under the terms and conditions of the Creative Commons Attribution (CC BY) license (<https://creativecommons.org/licenses/by/4.0/>).

1. Introduction

Sorafenib (SF) is a US Food and Drug Administration (FDA)-approved molecular-targeted chemotherapeutic agent [1–4], which is used as a clinic standard drug for hepatocellular carcinoma (HCC). The overall patient survival is increased by delaying the pathologic progression. SF is also an oral multikinase inhibitor by inhibiting the proliferation of tumor cells, neoplastic angiopoiesis, angiogenesis and invasion of cancer cells. So, SF is regarded as an effective chemotherapeutic agent against various types of tumors [5]. However, due to the high dose, poor solubility (25 ng/mL for SF free base in water), low bioavailability, dose-limiting side effects (diarrhea, anorexia, heart attack and infection, etc.) and possible drug resistance, the therapeutic application of SF is greatly restricted [6]. At the same time, pH-dependent SF is more soluble in an acidic environment because of the presence of amide and pyridine moieties. The aqueous solubility of commercial SF tosylate salt (Nexavar[®] by Bayer Pharmaceuticals, Leverkusen, Germany) is improved (65 ng/mL), but it is still poorly soluble in water [7]. Sorafenib tosylate has been authorized for renal cancer, hepatocellular cancer and differentiated thyroid cancer. The suggested dose in oral

usage is 400 mg, which is equivalent to two pills each day (200 mg/tablet) [8]. However, some shortcomings of sorafenib tosylate, such as low drug solubility, low drug permeability, cytotoxicity, side effects, and drug resistance across cancer cells, are still present.

Nanomedicine, via the delivery of drugs to tumor cells in a targeted fashion, is a promising strategy to solve these drawbacks [9,10]. Until now, the use of amphiphilic block copolymers as nanocarriers to generate colloidal delivery systems for hydrophobic drugs has been widely investigated. It is important to control particle size and distribution, morphology, zeta-potential, drug loading, encapsulation efficiency and process yield, which significantly affect drug pharmacokinetic properties, treatment outcome, biosafety, etc. There are distinct advantages such as: (1) carrying large amounts of drugs; (2) having prolonged circulation time; (3) facilitating selective tumor accumulation via the enhanced permeability and retention (EPR) effect; and (4) controlling drug release to target tissues. To achieve this aim, the entrapment of SF into nano-sized carriers affords SF-based nanomedicine, which is beneficial to reduce its side effects [11–16]. In this review, we focus on the recent advances of the nanocarrier-based delivery of SF (liposome, nanoparticle, micelle, emulsion, etc.) including preparation, mechanism of drug release, treatment efficiency and so on. The review is organized by type of carriers, including natural biomacromolecule (lipid, chitosan, cyclodextrin), synthetic polymer (poly(lactic-co-glycolic acid), polyethyleneimine, brush copolymer), mesoporous silica and others. Co-delivery of SF and other active agents (glypican-3, hyaluronic acid, apolipoprotein peptide, folate, superparamagnetic iron oxide nanoparticles) for targeted SF nanodrugs as well as other chemotherapeutic drugs are also highlighted (Figure 1), which show great potential to fight against various types of cancers. This review presents the latest advances, outlook, challenges and future opportunities in SF-loaded NPs to improve cancer treatment. We hope this review provides an insight and prospects in the design and preparation of ideal SF nanoformulations for clinical cancer therapy.

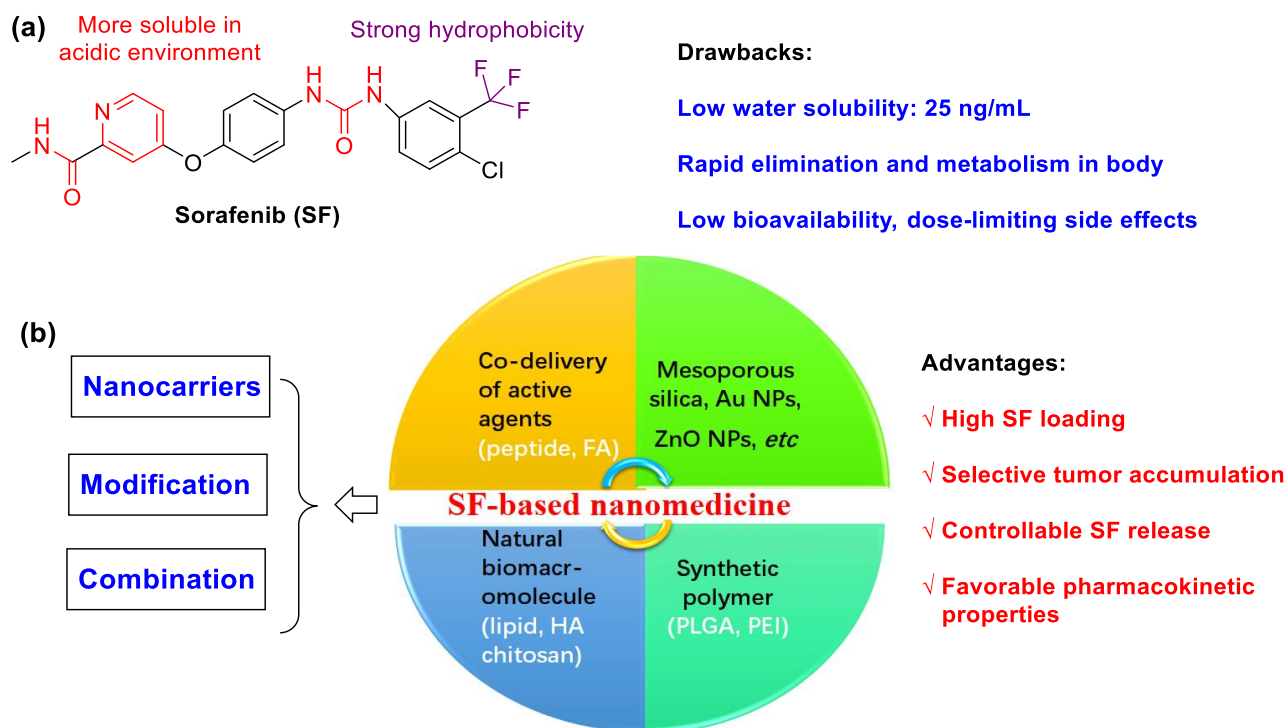


Figure 1. (a) The chemical structure of SF. (b) The design strategies of SF-based nanomedicine. Nanocarriers to improve release efficiency and bioavailability and actively target tumor tissues. Modification methods to increase the targeting and responsiveness of SF-based NPs. Combination therapies to Enhance treatment efficacy.

SF Inhibition Mechanism in HCC and Other Cancers

Three underlying mechanisms have been found to support SF inhibition mechanism in HCC [17]. First, SF blocks HCC cell proliferation by inhibiting BRAF and Raf1/c-Raf serine/threonine kinase phosphorylation in the mitogen-activated protein kinase pathway. Second, SF induces apoptosis by reducing eIF4E phosphorylation and downregulating Mcl-1 levels in tumor cells. Third, SF prevents tumor-associated angiogenesis by inactivating vascular endothelial growth factor receptors (VEGFR-2 and -3) and the platelet-derived growth factor receptor- β . In addition, SF is also shown to induce apoptosis through downregulation of Mcl-1 in many cancer types. Hence, SF as a single agent has shown promising activity in some cancers such as renal cell carcinoma (RCC) and thyroid cancers. Clinical trials have demonstrated the effectiveness and relative safety of SF, and thus, the drug is used in unresectable HCC. However, resistance to SF and serious side effect is shown by many patients. Many studies have combined SF with other treatments in an effort to increase its effects, reduce the necessary dose or overcome resistance.

2. SF-Based Nanomedicine

2.1. Biomacromolecule as Nanocarrier

As a kind of potential candidates for encapsulating hydrophobic drugs, nanostructured lipid carriers (NLCs) possess suitable size, good oral absorption, high biocompatibility, low toxicity and immunogenicity [18–21]. For example, the commercially pegylated liposomal doxorubicin (Doxil/Caelyx) and liposomal daunorubicin (Daunoxome, Galen) have been FDA approved as antitumor formulations. NLCs can be classified into solid lipid nanoparticles (SLNs) and liquid lipid nanoparticles (LLNs). The major difference between SLNs and LLNs is their lipid components. SLNs are prepared from solid lipids, whereas NLCs are modified by adding liquid lipids [20]. Both SLNs and LLNs are considered to be safe carriers since they are produced from physiological and biodegradable lipids. They can increase the stabilities of active ingredients and drug. However, LLNs exhibit higher drug loading capacities than SLNs, and lipid crystallization is avoided during drug storage because of the presence of liquid lipids, thus preventing drug expulsion. Until now, liposomes have been widely used as suitable nanovectors for the SF delivery since SF has high hydrophobicity and good lipid affinity.

Bondia and coworkers found that an NLC mixture (from solid and liquid lipids) would be a better nanocarrier than solid lipids alone, where higher drug loading capacity and longer-term stability were shown [22]. In vitro results indicated that more efficiently inhibited HCC cell growth than free SF (70% vs. 40% at 10 mM, and 85% vs. 55% at 20 mM) were obtained, leading to enhanced anti-tumor activity. When SF-loaded SLNs were prepared by combined high-speed shearing with ultrasonic treatment, high average encapsulation efficiency (EE) and drug loading (DL) of 89.87 and 5.39%, respectively, were shown [23]. Due to good liver-targeting capability, a 2.20-times higher average drug selectivity index value was found compared to that of the free SF-suspension. After oral administration, SF is metabolized in the mucosa of the small intestine and in the liver, where it is transformed into eight metabolites. When SF was encapsulated in SLNs matrix, SF was protected from metabolism or slowed down SF release from SLNs. Thus, SF remained in systemic circulation for a prolonged duration. Therefore, reducing the dosage of SF-SLNs could be considered to achieve the same pharmacological effects as the SF-suspension. As a result, a low side effect via oral administration was obtained by the protective lipid matrix and improved bioavailability.

The charged nucleolipids possess good stability, non-toxicity and self-assembly properties. Benizri et al. reported charged SF-loaded SLNs entrapped by nucleolipids with improved water solubility of SF (>120 μ M) and parallelepiped microstructure with 200 nm size [24]. Due to improved SF solubility, enhanced anticancer activities on four different cell lines (liver and breast cancers) were shown compared to free SF. Meanwhile, Ahiwale et al. used nanocarriers compressing 1,2-dioleoyl-sn-glycero-3-phospho-L-serine sodium salt and cholesterol for oral administration of SF tosylate [25]. The entrapment efficiency,

As a biodegradable, non-toxic and non-immunogenic protein, human serum albumin (HSA) is a promising carrier with multiple cellular receptors. Lactobionic acid (LA), the ligands for asialoglycoprotein (ASGP) receptors in HepG2 cells, was conjugated to HSA by amide bond formation between LA and HSA (Figure 3) [32]. The resulting LA-HSA conjugates were used as a targeted delivery system taking SF to HepG2 cells, which showed more cytotoxicity and cellular uptake than the untargeted ones with an IC_{50} value of 1.83 and 19.07 μM , respectively. The results indicated that LA as a targeting agent had a positive effect on tumor cell killing. Similarly, Gopakumar and coworkers showed core-shell protein nanoparticle as an albumin nanocarrier for SF showed a nearly two-fold enhancement in the oral bioavailability and enhanced therapeutic efficacy [33].

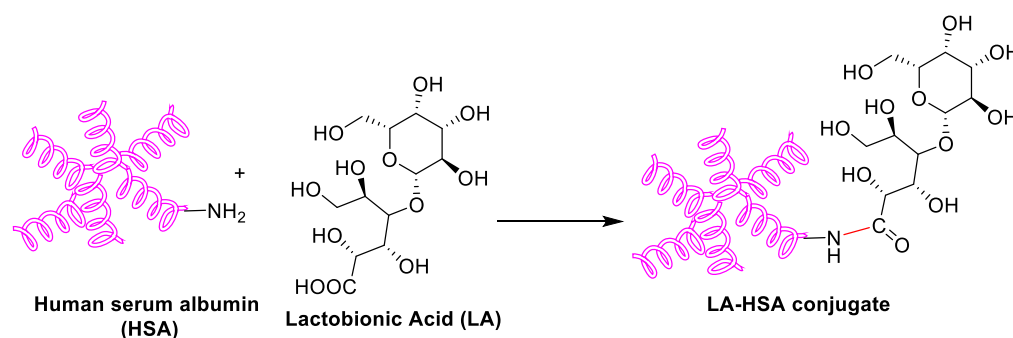


Figure 3. Schematic synthesis of LA-HSA conjugate.

Nonionic α -cyclodextrins (α -CD) are ideal carriers to deliver drugs [34]. Mazzaglia et al. reported supramolecular nanoassemblies based on α -CD and SF in aqueous solution for ablation of human HCC cells (Figure 4) [35]. The host-guest cooperation interaction between α -CD and SF produced highly water-dispersible colloidal nanoassemblies. The size of ~ 200 nm, negative zeta-potential ($\zeta = -11$ mV), maximum loading capacity ($\sim 17\%$) and entrapment efficiency ($\sim 100\%$) were found. There was a slower release of SF from nanoassemblies with respect to the free SF. In addition, nanoassemblies showed low hemolytic activity and a high efficiency to inhibit the growth of three different HCC cell lines.

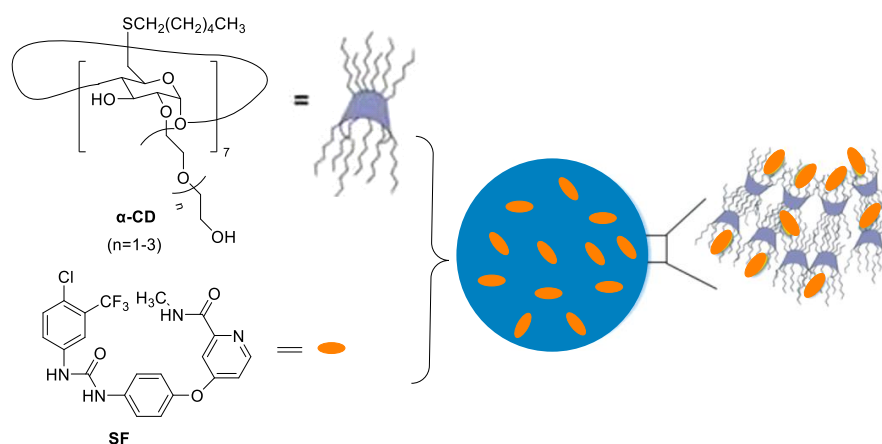


Figure 4. The supramolecular nanoassemblies based on α -CD and SF in aqueous solution.

As a natural anionic polysaccharide, hyaluronic acid (HA) directly binds to CD44, and RHAMM receptors overexpressed on various tumor cell surfaces. Mo et al. reported PEGylated HA-coated liposome for enhanced SF delivery and anti-tumor outcome via active tumor cell targeting and prolonged systemic exposure [36]. For MDA-MB-231 cells over expressing CD44, greater cellular uptake and cytotoxicity were found. However, there were no significant differences in MCF-7 cells with low CD44 expression. Compared with

SF solution, PEG-HA-SF-Lip increased the systemic exposure and plasma half-life in rats by 3-fold and 2-fold, respectively. The effective tumor growth inhibition through CD44 targeting in the MDA-MB-231 tumor xenograft mouse model was demonstrated.

SF and cisplatin (*cis*-Pt) are two chemotherapeutic drugs with different antitumor mechanisms. Zhang et al. developed pH-sensitive hyaluronic acid NPs encapsulating with SF and *cis*-Pt, where interactions between cisplatin and HA was involved [37]. The pH-sensitive property guaranteed the effective release of loaded drugs (*cis*-Pt and SF) in tumor sites. The HA@*cis*-Pt@SF showed prolonged circulation time and high accumulation rate, leading to exerted synergistic tumor-killing effects.

2.2. Synthetic Polymer as Nanocarriers

Poly(lactic-co-glycolic acid) (PLGA) is approved by the FDA as a drug carrier due to its hydrophobic properties and biocompatibility. Kim et al. prepared hydrophilic dextran-conjugated PLGA (PLGA-Dex, Figure 5a) [38]. In this case, dextran and PLGA acted as a hydrophilic and biodegradable hydrophobic domain, respectively. The SF-incorporated PLGA-Dex NPs were fabricated via the nanoprecipitation–dialysis method. The loading efficiency was higher than 35%. An initial burst of release and a sustained release of SF was observed. A dose-dependent antiproliferative effect against HuCC-T1 tumor cells was shown. In 2016, to regulate size polydispersity and the stability of NPs in the blood circulation, a mixture of amphiphilic copolymer of poly(ethylene glycol)-*b*-PLAG and PLGA (5/5) was co-formulated to entrapped SF [39]. The blood circulation of the cargo was significantly prolonged, resulting in increased uptake by liver fibrosis in CCl₄-induced fibrosis models. In particular, vessel normalization in the fibrotic livers was observed.

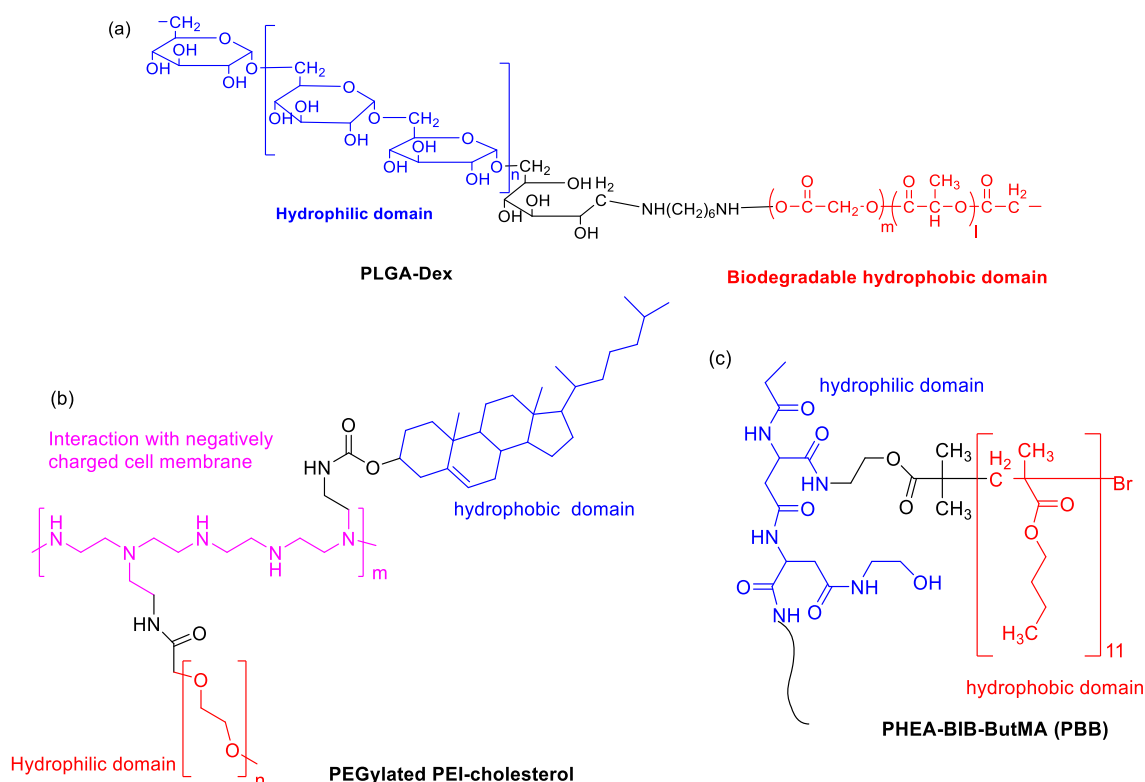


Figure 5. The chemical structures of (a) PLGA-Dex, (b) PEGylated PEI-cholesterol and (c) PBB.

Due to the presence of primary, secondary and tertiary amines in the polymer structure, cationic polyethyleneimine (PEI) exhibits “proton sponge” effect by interaction with negatively charged cell membrane. PEGylated PEI-cholesterol lipopolymers (Figure 5b) were synthesized, where cholesterol functionalization was helpful for endocytosis, enhancement of drug loading capacity and reduction in the drug burst release [40]. When they

were used as nanocarriers, SF-loaded NPs exhibited maximum drug loading ($13.1\% \pm 2.65$) and concentration-dependent toxicity by pharmacological action through the charge shielding mechanism.

An amphiphilic brush copolymer PHEA-BIB-ButMA (PBB, Figure 5c) was synthesized by Atom Transfer Radical Polymerization (ATRP) [41]. SF was entrapped into its inner hydrophobic core in an aqueous environment as a drug reservoir. The spherical morphology (200 nm size), negative ζ potential and sustained SF release capability was found. Compared to free drug, SF-loaded NPs showed a higher inhibition efficacy of tumor growth and more accumulation in the solid tumor mass in *in vivo* xenograft models.

Liquid crystalline nanoparticles (LCN) have high stability, sustained drug release, and high drug payload to the target site [42]. Thapa et al. prepared a pH-responsive polymer-coated LCN with poly-L-lysine (PLL) and poly(ethylene glycol)-*b*-poly(aspartic acid) (PEG-*b*-PAsp) for SF delivery [11]. Due to selective depolymerization of polymer layers by acidic tumor microenvironment, the pH-responsive SF-loaded nanomedicine showed enhanced drug release. As a result, the intracellular uptake of SF was significantly improved, generating better antitumor efficacy against HepG2 cells.

The amphiphilic polymer based on polyacrylic acid (PAA) with D- α -tocopherol succinate (VES) via a disulfide bond linker was synthesized [43]. SF was entrapped in the polymer micelles, where the release of SF was dependent on the concentration of glutathione (GSH) because of GSH sensitivity of disulfide linkage. A 2.8-fold bioavailability of SF was achieved by injecting the animal compared with free SF by this redox-responsive SF delivery system.

To control particle morphology, size distribution and reproducibility from batch-to-batch, a microfluidic process with glass-based microcapillary devices was developed for preparation of micellar-like PEG-*b*-PCL NPs loaded with SF free base [44]. Under optimized nanoprecipitation process, spherical NPs with loading degree (16%), encapsulation efficiency (54%), particle size less than 80 nm were obtained. More importantly, 20,000-fold increase in solubility was achieved as compared to free SF in PBS. They found process temperature, flow rate, nanoprecipitation temperature, and organic solvent removal method had the significant effects on particle size distribution, morphology distribution, zeta-potential, drug loading, encapsulation efficiency and process yield. The *in vitro* drug release study indicated that SF was released from the NPs in a sustained manner, where 13.6% and 25.3% release rate in 8 and 24 h at pH 7.4 was shown.

Colorectal cancer has overexpressed matrix metalloproteinase (MMPs), especially MMP-2. The MMP-2 responsive nanocarrier assembled by amphiphilic polyethylene glycol (PEG)-peptide copolymer for simultaneously loading camptothecin and SF for combination therapy (Figure 6) [45]. Two drugs were released upon exposure to tumor microenvironment because the peptide segments could be digested by MMP-2, leading to higher synergistic efficacy than that of single antitumor agents. The photoacoustic (PA) imaging signals kept constant for the whole week during detection the angiogenesis of *in vivo* HT-29 bearing mice.

2.3. Inorganic and Metal Nanocarriers

Hollow mesoporous silica nanoparticles (MSNs) show uniform particle size distribution, excellent water dispersion, large specific surface area and good biocompatibility [46], which are ideal drug delivery nanocarriers [47]. Shao's group reported a series of MSNs-based SF NPs [48,49]. For example, MSNs were used as nanocarriers for the co-delivery of SF and siRNA, leading to enhanced cytotoxicity and improved the tumor target of SF in asialoglycoprotein receptor (ASGPR)-overexpressing Huh7 cells [48]. Since lactobionic acid (LA) could target human HCC effectively, an ASGPR-targeting SF delivery system based on MSNs co-delivery of vascular endothelial growth factor (VEGF)-targeted siRNA (siVEGF) and LA was synthesized as follows [48]. NPs based on MSN-NH₂ and SF were fabricated by non-covalent interactions. Then, LA was chemically linked to the surface of the NPs. Finally, siVEGF were loaded into the nanocarrier by electrostatic interaction.

The improvement in the targeting property resulted in enhanced anti-cancer efficacy of SF. Recently, SF was loaded into manganese-doped MSNs by physical adsorption [50]. In this case, high-concentration GSH could break manganese-oxidation bonds leading to the degradation of MSNs. This dual GSH-exhausting (consumption or synthesis inhibition of GSH) nanomedicine showed a significantly enhanced in vitro inhibitory effect.

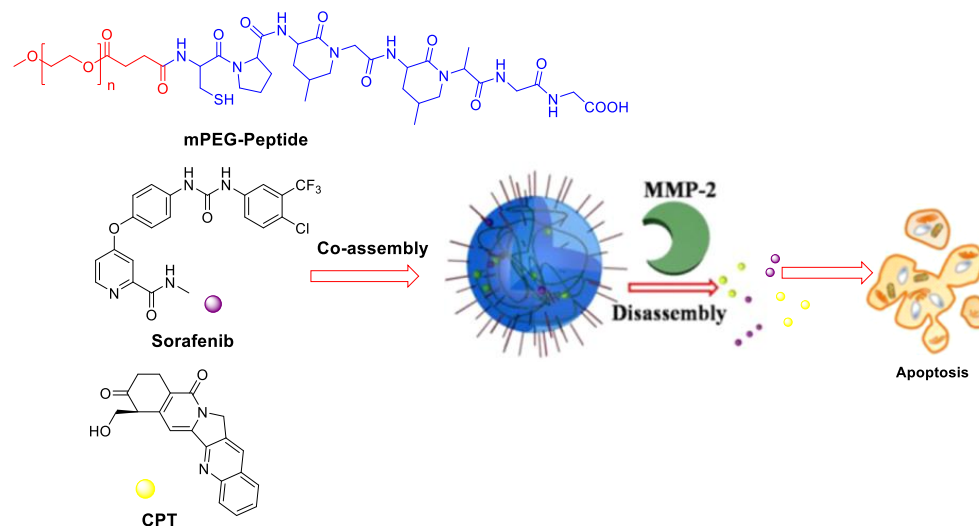


Figure 6. MMP-2-responsive nanoparticles for synergistic antitumor effect of anti-angiogenesis and chemotherapy. Adapted with permission from [45]. Copyright 2016, American Chemical Society.

To decrease the risk of post-surgical HCC relapse, a wound-targeted nanodrug containing immune checkpoint inhibitor (anti-PD-L1) and SF as an angiogenesis inhibitor was developed, where a mesoporous silica with a surface-coated platelet membrane as surgical site-targeting nanocarriers was used [51]. The resulting nano-formulation efficiently inhibited post-surgical HCC relapse without obvious side effects.

Gold NPs with high biocompatibility and negligible toxicity, small size and precise targeting ability are suitable candidates for a drug delivery system for the treatment of various diseases. FA-*b*-PEG-modified gold NPs loaded with SF tosylate were fabricated, providing an effective treatment for retinal neovascularization in patients of diabetic retinopathy [52]. MiR-221 plays a role in promoting tumorigenesis in HCC by inhibiting the expression of p27. Cai et al. investigated the synergistic anti-tumor effects of SF and gold NPs-loaded anti-miR221, leading to a strong synergistic effect on inhibiting proliferation of HCC cells [53]. Recently, alginate/CaCO₃ hybrid loaded with SF tosylate and gold hexagons was developed for the dual (chemo-radio) treatment of HepG2 cells [54].

As a versatile inorganic compound, sodium selenite (Na₂Se) NPs exert anticancer effect by inducing apoptosis. A co-delivery system for SF and Na₂Se was prepared when tripolyphosphate was used as a crosslinker via the solvent evaporation technique [55]. The resulting NPs had a zeta potential of −37.5 mV and size (diameter) in the range of 208 nm to 0.2 μm. The sustained release of the drug to elicit synergetic action was developed. Selenium NPs have distinct characteristics of high biocompatibility, low-toxicity and degradability in vivo, and radiosensitization effects with X-ray. An injectable thermosensitive nanosystem based on SF, Se NPs and PLGA-PEG-PLGA was prepared [56]. When it was injected in HepG2 tumor-bearing nude mice, the resulting hydrogel for long-acting therapy with the degradation of PLGA-PEG-PLGA was obtained. The raised expression of cleaved caspase-3 in tumor tissue was observed based on the synergistic local treatment and chemoradiotherapy.

ZnO-NPs possess excellent physicochemical properties of safety, biodegradability, fast delivery rate and cytotoxicity against tumor cells [57]. ZnO-NPs might be a safe candidate in combination with SF to generate enhanced treatment effect [58].

2.4. Co-Delivery of SF and Other Drugs

The SF-based monotherapy is often hampered by its modest efficacy, severe systemic toxicity and high occurrence of drug resistance. In order to enhance the antitumor effect of SF and reduce its side effects, different drugs are co-loaded in nanomedicine. Doxorubicin (DOX) is an effective chemotherapy agent, but it suffers from some drawbacks such as low response rate, severe side effects and cytotoxicity to normal tissues. Although DOX and SF have completely different chemical characteristics, Babos et al. reported the entrapment of DOX and SF by PLGA/PEG-PLGA using the double emulsion solvent evaporation method [59]. The DOX-SF NPs showed a suitable size (~142 and 177 nm), high drug encapsulation efficiency (69% for DOX and 88% for SF) and high drug loading. The DOX was released continuously within 6 days, while the SF was released quickly during 24 h under biorelevant conditions. Duan et al. formulated a specific sugar-modified pH sensitive lipid system for the co-delivery of DOX and SF for combination HCC chemotherapy [60]. In this case, DOX prodrug (NAcGal-DOX, Figure 7) contained pH-sensitive hydrazine moiety and N-acetylgalactosamine, allowing a rapid DOX release at the tumor site and targeting to highly expressed asialoglycoprotein receptors in HCC. DOX and SF were entrapped by single-step nanoprecipitation in the presence of soya lecithin and polysorbate 80. The targeted ability of sugar to HCC and strong synergy between DOX and SF generated a higher anti-tumor efficiency of drugs.

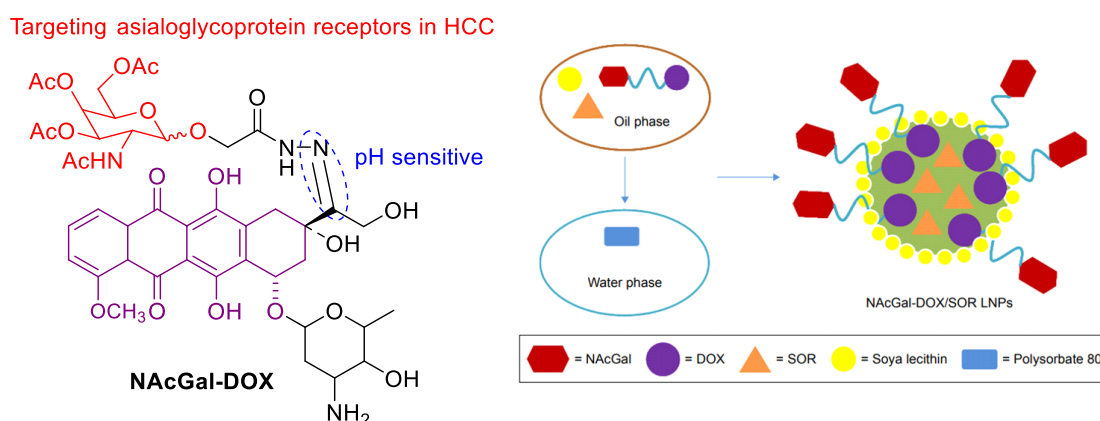


Figure 7. The chemical structure of NAcGal-DOX and co-loading in NAcGal-DOX/SF NPs.

In order to deliver SF in a targeted fashion into undifferentiated/anaplastic thyroid carcinoma cells, Mato et al. developed SF-loaded PLGA NPs covalently attached with cetuximab [61]. SF-loaded PLGA NPs were firstly prepared by the single emulsion evaporation method. Then, EDC/Sulfo-NHS cross linking chemistry was utilized to conjugate cetuximab to SF-loaded PLGA NPs, yielding 51% cetuximab incorporation. The resulting NPs showed suitable size (252 nm) and drug entrapment efficiency (58%). A higher specificity to the anaplastic cells line (CAL-62) that overexpress EGFR was shown, providing a promising targeting approach for the treatment of epithelial thyroid cancer.

Recently, SF and all-trans retinoic acid (ATRA), a differentiation-promoting drug, were loaded into PEG-PLGA polymer micelles [62]. The two drugs-loaded micelles exhibited relatively slow drug release and effective cell uptake, yielding significant antitumor effect and minimal systemic toxicity toward the FTC-133 thyroid cancer-bearing BALB/c nude mouse model.

Combretastatin-A4 (CA4) is a representative vascular disrupting agent (VDA) which causes significant central tumor necrosis by selectively arresting tumor blood flow and disrupting the established tumor vasculature. Wang and coworkers prepared NPs of poly(L-glutamic acid)-graft-methoxy poly(ethylene glycol)/combretastatin A4 sodium salt (CA4-NPs) via a Yamaguchi reaction and following salination reaction [63]. The combination of SF 30 mg.kg⁻¹ + CA4-NPs 30 mg.kg⁻¹ (on the CA4 basis) showed an over 90% tumor suppression rate in a hepatic H22 subcutaneous tumor model with low systemic

toxicity. A total of 71% of treated mice survived in tumor-free state for 96 days. These findings indicated that the two-pronged attack of SF and CA4-NPs (as a tumor blood-flow reducer) was a promising therapeutic approach for HCC treatment.

The combination of SF and Bosutinib drug was co-loaded in a self-emulsified drug delivery system [64]. The superior antitumor treatment effect for HCT116/SW1417 by destroying the DNA structure to inhibit cell proliferation was shown. Yin et al. formulated liposomes entrapping ceramides and sorafenib and showed a synergistic cytotoxic effect on HepG2 when compared to single-drug liposomes [65].

Most nanoformulations focus on one nanocarrier for one drug. Sukkar et al. investigated a comparative study on two polymeric nanocarriers for SF against HepG2 Cells [66]. In this study, two biocompatible polymers (PLGA or PCL) were used for the co-delivery of SF tosylate and gold nanoparticles (G), where the latter was selected as a radiosensitizer. SF/PCL NPs showed slower SF release rate than SF/PLGA NPs (27.9% vs. 31.2% in pH = 7.2 and 46.3% vs. 61.3% in pH = 5.2). Both SF/PCL/G NPs and SF/PLGA/G NPs exhibited elevated necrosis and apoptotic levels through the synergistic combined chemo–radio treatment. The IC₅₀ values for SF/PCL NPs, SF/PLGA NPs, SF/PCL/G NPs, and SF/PLGA/G NPs were found to be 12.7, 10.3, 8.9, and 4.9 µg/mL, respectively.

2.5. Imaging-Guided SF Nanodrugs

Nanomedicines combining drug delivery and imaging functions have been employed as theranostic tools for imaging-guided cancer therapy. Superparamagnetic iron oxide nanoparticles (SPIONs) are suitable nanocarrier systems for cancer therapeutics [67–69]. SPIONs within the lipid matrix were used to construct magnetically responsive SLNs. Grillone et al. developed SF-loaded magnetic SLNs (SF-Mag-SLNs) to enhance SF delivery with the help of a remote magnetic field using cetyl palmitate as lipid matrix [70]. The resulting NPs had a 90% SF loading efficiency, a regular spherical shape and an average diameter of less than 300 nm. SF-Mag-SLNs were able to inhibit cancer cell proliferation through the SF cytotoxic action. Good targeting properties and attenuated side effects were achieved via a magnetically driven accumulation of SF. However, the preparation process is extremely complex and tedious.

The use of poly(vinyl alcohol)-coated SPIONs as a polymeric-magnetic delivery system for SF with significantly enhanced activity was developed via co-precipitation and physical entrapment methods [71]. An entrapment value of 76.37% and a release rate of SF up to 66.7% in 80 h were obtained. The MTT assay showed that the cytotoxicity of SF-loaded PVA/SPIONs was comparable or higher than that of free SF. The apoptosis study in HepG2 cells indicated that the combination of SF with PVA/SPIONs showed a higher percentage of early apoptotic cells than free SF (13.8% vs. 11.4%).

A reduction and pH dual-sensitive nano-formulation co-encapsulating SPIONs and SF was developed and further functionalized by anti-GPC3 antibody (AbGPC3) for magnetic resonance imaging (MRI)-monitorable HCC-targeted therapy [72]. The AbGPC3-mediated active targeting enhanced cancer cell uptake and tumor accumulation of nanodrug. Consequently, the nanodrug displayed prominent anticancer effects (the lowest tumor weight was only 12.3% of that for the saline group) in an animal study via responding to the cytoplasmic glutathione and lysosomal acidity. Moreover, tumor detection and monitoring of drug delivery process by MRI were obtained.

Faramarzi et al. developed functionalized magnetic nanoparticles with chitosan for adsorption of SF and thermosensitive N-isopropylacrylamide to control release (Figure 8) [73]. The radical copolymerization of allyl glycidyl ether (AGE), N-isopropylacrylamide (NIP) and silica-coated magnetic NPs was firstly involved. The following coupling reaction between chitosan and epoxy ring of the AGE afforded thermosensitive magnetic nanocarrier (TSMNC). Due to superparamagnetic properties, rapid adsorption and slow release at low and high temperatures, Fickian diffusion-controlled drug release was obtained, where about 88% of SF was released within 35 h at 45 °C. Recently, SF tosylate-loaded

PCL-superparamagnetic nanoparticles were prepared by an emulsion solvent evaporation method and optimized using Box–Behnken design [74].

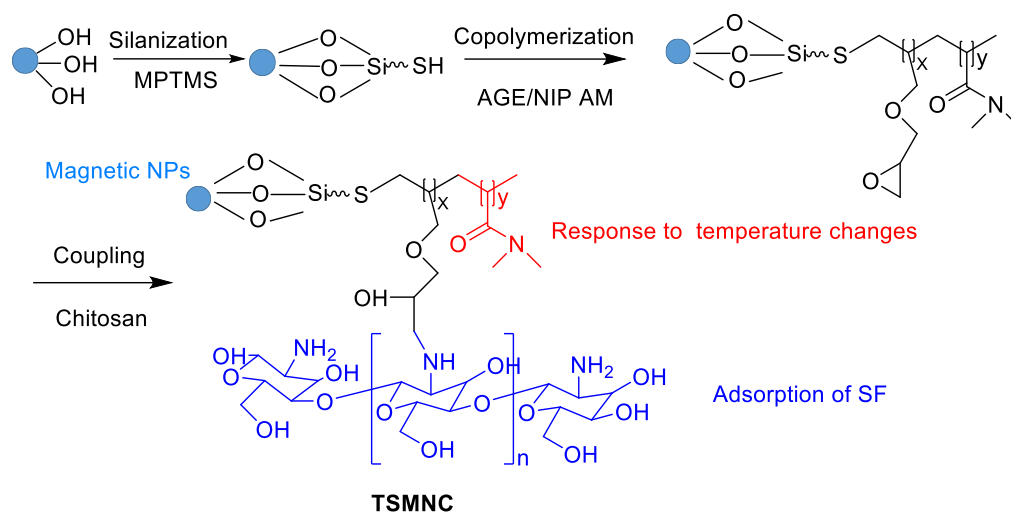


Figure 8. Synthetic route of TSMNC.

Zhang et al. prepared SF and gadolinium (Gd) co-loaded liposomes (SF/Gd-liposomes) using Lipoid E80 and cholesterol as carriers for MRI-guided visualization of the delivery and HCC treatment [75]. The solubility of SF in SF/Gd-liposomes was significantly increased to 250 ng/mL. SF/Gd-liposomes exhibited spherical shapes or ellipsoidal shapes, uniform particle size distribution, negative zeta potential, high encapsulation efficiency and drug loading. Due to its limited drug release and slower absorption by HepG2 cells, lower cell cytotoxicity from SF/Gd-liposomes was observed. In the MRI test, longer imaging time and higher signal enhancement were obtained at the tumor tissue.

Manganese dioxide (MnO_2) nanosystems can react with H^+ and glutathione (GSH) in the tumor microenvironment (TME) [76]. The resulting paramagnetic Mn^{2+} significantly increases the contrast of T_1 in MRI, which is useful for tumor-specific imaging and multifunctional drug carrier systems [77]. Wang et al. reported aptamer-mediated hollow MnO_2 for targeting the delivery of SF, where aptamer could specifically bound to glypican-3 (GPC3) receptors on the surface of HCC [78].

A dicarboxylic acid-containing ICG was selected as a NIR photosensitizer and fluorescent dye, which was co-loaded with SF by Pluronic F127 to produce self-assembled and self-monitored nanodrug [79]. Through a strong hydrogen bond between the carboxyl group of ICG and the urea bond of SF, stable nanodrug with a particle size of ~70 nm was formed. Due to optimal physical and chemical characteristics, nanodrugs had a longer blood retention time (up to 36 h) and preferable tumor accumulation, thereby yielding ultrasensitive NIR-II fluorescence images and photothermal tumor ablation ($\Delta T = 25^\circ\text{C}$) in *in vivo* nude mice bearing Huh7 tumor. The combination of photothermal therapy and chemotherapy based on ICG and SF would offer potential for HCC treatment since two drugs and Pluronic F127 have been widely used in the clinic.

Liu et al. designed a new nanocarrier platform for SF delivery, where the tumor chemotherapy process was guided and evaluated by NIR-II dual-modal optical coherence tomography and photoacoustic imaging [80]. Because integrin $\alpha_v\beta_3$ is regarded as the targeted site for HCC, arginine–glycine–aspartic acid (RGD) functionalized carriers are promising. The multifunctional SF theranostic nanosystems were prepared based on cyclic RGDfK and S-Cy5.5 fluorescent dyes-functionated PEG-PCL for fluorescence imaging-guided HCC treatment [81].

2.6. Actively Targeted Nanosystems

Feng et al. designed a lipid-coated nanocarrier functionalized with peptides specific for glypican-3, which showed targeted drug delivery to human HCC xenograft tumors [82]. PLGA and 1,2-dioleoyl-snglycero-3-phosphocholine (DOPC) were utilized as a hydrophobic core to entrap SF and as a lipid shell to prevent drug leakage, respectively (Figure 9). The peptides are attached to the nanocarrier surface via a thioether-mediated conjugation. The entrapment efficiency (%EE) for SF was > 80% with concentrations up to 69.5 mg/L, which showed a 1900-fold improvement in aqueous solubility versus free SF. The half-life release ratio in vitro was 22.7 h. The greater tumor regression was shown due to the target peptide versus controls after 21 days of therapy.

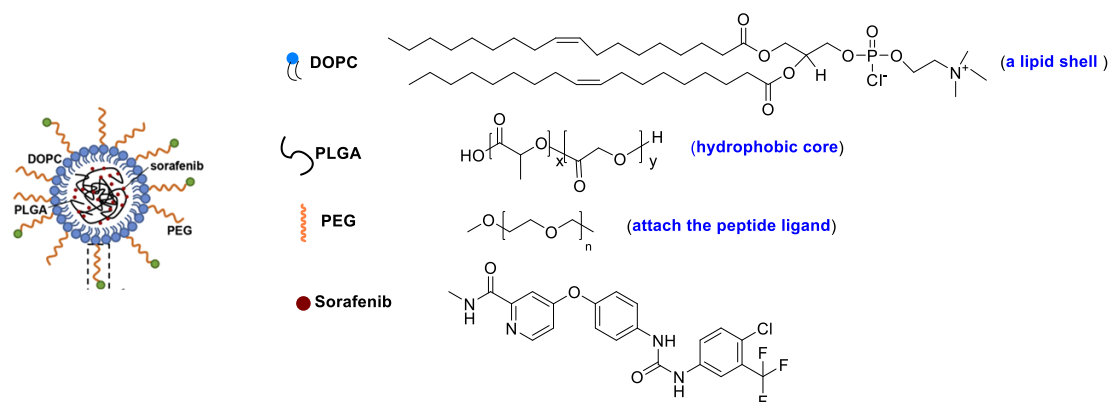


Figure 9. A lipid-coated nanocarrier.

SLN appended with PEGylated galactose (Figure 10) was developed to modulate the site-specific oral delivery of SF for HCC treatment because galactose is a C-type lectin receptor binding ligand [83]. The encapsulation of SF into SLN and use of PEGylated galactose as targeting ligand provided a liver-targeting, biocompatible drug delivery system and increased circulation half-life. The oral bioavailability of the SF can be improved by encapsulating it in SLN and grafting it with PEGylated galactose.

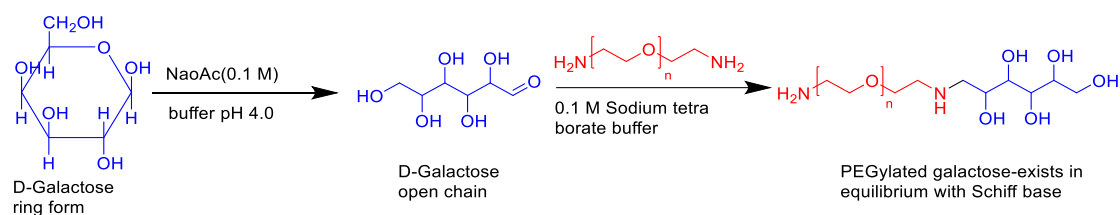


Figure 10. The synthetic route of PEGylated galactose.

Zhong et al. reported a redox-responsive SF delivery system based on apolipoprotein E peptide-decorated disulfide-cross-linked polymer and SF by self-assembly and self-crosslinked process [84]. The resulting NPs exhibited a good SF loading of 7.0 wt%, a small size (37 nm) and high stability. Due to presence of a disulfide bond, reduction-triggered drug release from polymer nanocarrier, a long circulation time and enhanced SF therapy for orthotopic HCC in mice were shown. AMD3100 possess anti-tumor activity upon combination with chemotherapy. The resistance to anti-angiogenic therapy of HCC by SF is activated by C-X-C receptor type 4 (CXCR4). Chen et al. co-delivered SF together AMD3100 attached to lipid-coated PLGA NPs [85]. They demonstrated that CXCR4-targeted NPs efficiently delivered SF into HCCs and human umbilical vein endothelial cells (HUVECs) to achieve cytotoxicity and anti-angiogenic effect in vitro and in vivo.

Folate (FA) can enter cells through a receptor-mediated endocytosis pathway. It is highly expressed in tumor tissue at a level 100–300 times higher than that in normal tissues. The FA receptor is a good target for targeting delivery systems for many solid tumors.

Zhang et al. prepared FA-functionalized polymeric micelles loaded with SPIONs and SF, which can increase the concentration of SF in HepG2 cells [86]. Li et al. developed SF/FA/PEG-PLGA NPs with both anticancer and magnetic resonance properties, which can improve the antitumor activity in vitro [87]. In 2019, Xie et al. developed bovine serum albumin (BSA) modified with FA by chemical coupling as the drug carrier (Figure 11) [88]. Good stability for more than 1 month at room temperature was found. The average particle size (158 nm), zeta potential (-16.27 mV), entrapment efficiency (77.25%), and drug loading (7.73%) were obtained. As compared with SF-BSA NPs and SF solution, SF-BSA-FA NPs showed the best intracellular uptake of hepatoma cells (SMMC-7721) and the strongest inhibitory effect. Moreover, excellent tumor targeting ability with higher $C_{\text{tumor}}/C_{\text{blood}}$ value (0.66) than those of the former two (0.56 and 0.41) in a nude mice liver cancer model were found.

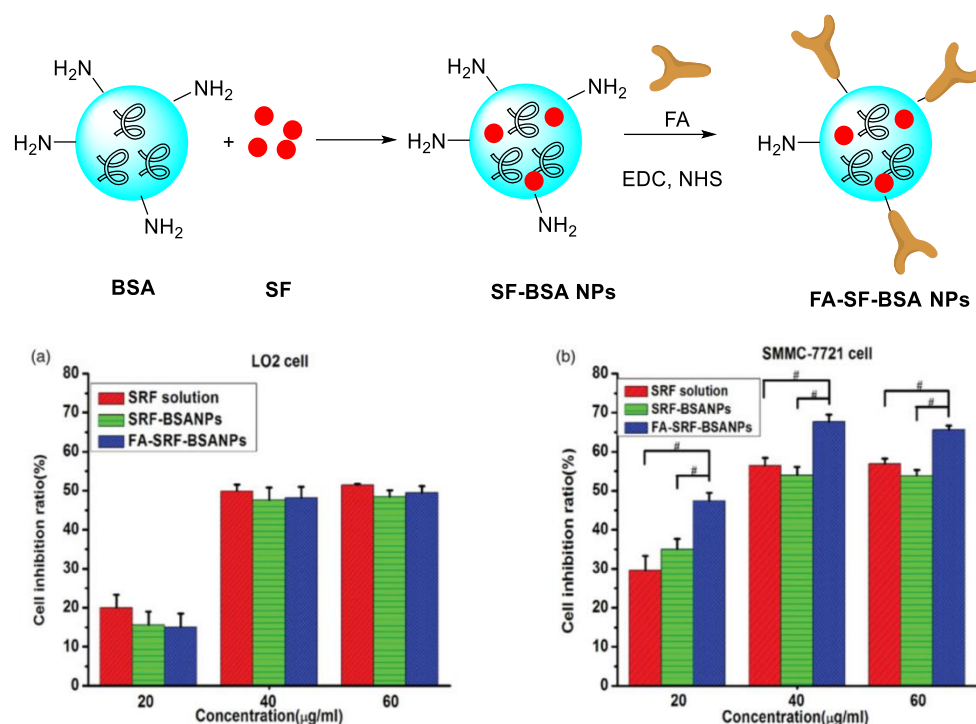


Figure 11. Schematic synthetic route of SF/FA/PEG-PLGA NPs. Cell inhibition ratio on three concentration levels of SF solution, SF-BSA NPs, and FA-SF-BSANPs against (a) LO2 cell lines or (b) SMMC-7721 cell lines after incubation for 24 h [88]. # indicates a statistically significant difference between two groups $p < 0.05$, independent sample t -test. Copyright 2021, Taylor & Francis.

FA-modified PEG-nitroimidazole grafts exhibited a targeting SF delivery ability in the treatment of hypoxic HCC [89]. Since antibody hGC33 has important antitumor activity, Shen et al. described hGC33-modified PEG-b-PLGA for SF delivery to increase the targeting to HCC cells [90].

The presentative SF-based drug delivery systems are summarized in Table 1.

2.7. Combination of Ferroptosis and Others

Ferroptosis is an alternative to the traditional apoptotic pathways for cancer therapy, which is regarded as an iron-based Fenton-type reaction. Since SF can induce the occurrence of ferroptosis, some combinational therapy methods have been proposed [91]. Zhou et al. described a metal-polyphenol network-based SF nanodrug for combinational ferroptosis and PDT, showing a more excellent inhibitory effect on tumor cells [92].

The novel drug-mate strategy has been developed in the nanomedicine field. Namely, amphiphilic small molecule and hydrophobic drugs with poor solubility are selected as a mate and drug, respectively (Figure 12). Taking SF/D- α -tocopherol succinate nanoassem-

blies as an example, drug loading content (46%) was shown compared with the lipid-based SF nanodrugs (11%) and SF liposomes (4%) [93]. The highest SF water dispersion was due to stronger interaction between small molecular mate (SMA) and SF than that between SF itself. In vitro cytotoxicity assay indicated the IC₅₀ of SF NPs based on the drug–mate strategy was close to that of free SF (3.44 vs. 4.44 µg/mL). However, the pharmacokinetics of the former were largely improved, where the plasma concentrations of SF was 2 and 20 times than that of the SF solution and SF suspension, respectively. In vivo antitumor efficacy study further revealed the increased bioavailability and enhanced therapeutic efficacy of SF.

Table 1. The presentative SF-based drug delivery systems.

NPs	Average Particle Size (nm)	Zeta Potential (mV)	Entrapment Efficiency (EE%)	Drug Loading (DL%)	Application	Ref
Cyclodextrin @SF	200	−11	100	17	HCC cell line	[35]
PEI-cholesterol @SF	30	12.4	-	13.1	HepG2 cells	[40]
PLGA@ cetuximab @SF	277	−11.1	-	-	CAL-62 and Nthyori 3-1 cell	[61]
PEG-PLGA @SF	230	-	-	15%	IC ₅₀ : 2.6 µM (HSC); IC ₅₀ : 1.6 µM (HUVEC); liver fibrosis of C3H mice	[39]
Glypican-3@SF	114	−20.9	>80%	[SF]: 69.5 mg/L, T _{1/2} = 22.7 h	HCC cells in vitro, growth inhibition of HCC tumors	[82]
SPIONs @SF	5–15	-	76.37%	-	HCC cells, Wistar rats	[71]
PEGylated galactose @SF	111	−19.8	95	-	HepG2 cells and BALB/c mice	[83]
lipid@SF	221	−37	100	18.46	Four different HCC cell lines	[22]

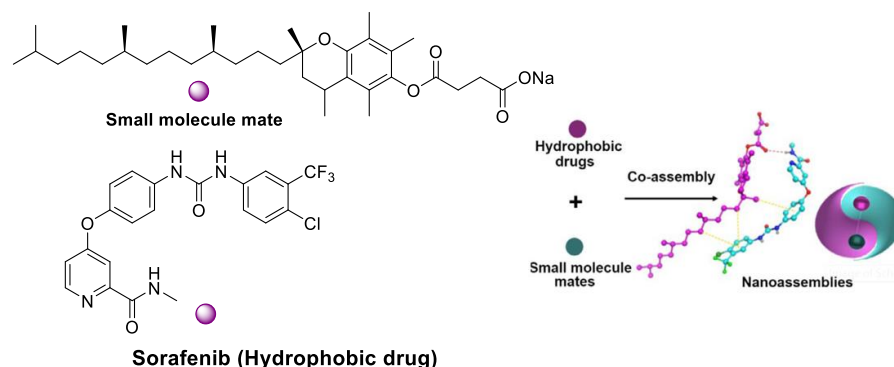


Figure 12. SF/D-α-tocopherol succinate nanoassemblies based on the drug–mate strategy.

3. Challenges and Opportunities

With the development of nanotechnology, nanocarrier-based SF delivery systems have been widely studied. Its poor pharmacokinetic properties have been improved to some extent. The synergistic drug combinations also exhibit potential for cancer treatment due to their superior therapeutic benefits to the classical monotherapeutics. The innovative optimization of nanocarriers structures (modulation of particle size, an increase

in particle-specific surface area, multifunctional surface modification, etc.) improves the bioavailability and therapeutic efficiency of anti-tumor drugs. The chemical and physiological properties of nanocarriers largely affect the synergistic actions combined drugs. However, some challenges still exist such as low drug loading, uncontrollable drug release, insufficient tissue penetration, loss of targeting ability, biosafety, etc. In particular, ligand- or surface-modified nanocarriers are utilized to enhance the SF anti-tumor effect. According to the receptors over-expressed on the surface of tumor cells, specific ligands, such as antibodies, proteins, peptides, aptamers or folic acid, were introduced for the surface modification of nanocarriers to achieve active targeting via biological substrate/receptor (antibody/antigen) recognition. However, the “overexpression” of relevant receptors on the surface of tumors is not sufficient to impart high selectivity due to tumor heterogeneity. Moreover, the development of nanoformulation often requires complex nanocarrier synthesis/modification, purification and fabrication. Some shortcomings such as stability, handling inconvenience, blood stability, reproducibility from batch-to-batch and scale-up issues are encountered. The reproducibility from batch to batch is also a problem. Most SF-based nanodrugs are studied at the cellular and animal level. There are various physiological barriers in terms of clinical translation.

4. Conclusions

The selection of nanocarriers for SF delivery is essential to improve its biopharmaceutical properties. Various types of representative materials such as lipid- and polymer-coated nanomatrix, natural and synthetic polymeric, MSNs, pH- or GSH- responsive NPs, gold NPs, injectable sodium selenite NPs and in situ gel with lipid coating are utilized to promoting SF nanoformulations. The bioavailability, solubility, drug targeting and cytotoxicity of SF are improved, which is facile for circumventing some of the unfavorable outcomes of traditional SF regimens. SF-based nanodrugs cannot stay in the tumor site for a longer period when they enter the blood circulation by diffusion and via the ERP effect. Moreover, some nanocarriers are difficult to be removed from the blood stream due to high physicochemical stability and unsuitable particle size, which may increase systemic toxicity and organ damage. Appropriate surface modifications could enhance the localization and specific accumulation of nanocarriers in tumor cells by ligand–receptor interactions. Studies have shown that precise targeting of receptors on tumor cells or tumor vessels by ligand-modified nanocarriers can improve the efficacy of drugs. The application of biodegradable nanocarriers would be a promising strategy to control toxicity and improve biological compatibility. In the future, more attention should be paid to the surface characteristics, biosafety, targetability by connecting tumor-targeting ligands, controlled release with stimuli-responsive linkers, and so on. Moreover, it is important to combine SF with other treatments for synergistic therapy (chemotherapy, immunotherapy, photodynamic therapy, photothermal therapy). Scientists should make more efforts to investigate the biodistribution, pharmacokinetic response and in vivo efficacy of various SF nanoformulations. All in all, SF nanoformulations hold great potential and prospects in cancer therapeutics in the future. It is urgent to study the mechanisms underlying how SF interacts with cellular molecules and other drugs to increase its efficacy and reduce resistance in HCC patients.

Author Contributions: Conceptualization and supervision, L.W.; investigation and writing, M.C.; editing, X.R., H.T. and D.C.; All authors have read and agreed to the published version of the manuscript.

Funding: This research was funded by National Natural Science Foundation of China (22071065) and Natural Science Foundation of Guangdong Province (2022A1515011743).

Institutional Review Board Statement: Not applicable.

Data Availability Statement: Not applicable.

Acknowledgments: We are grateful to the National Natural Science Foundation of China (22071065) and Natural Science Foundation of Guangdong Province (2022A1515011743) for the financial supports.

Conflicts of Interest: The authors declare no conflict of interest.

References

1. Zhang, X.; Yang, X.R.; Huang, X.W.; Wang, W.M.; Shi, R.Y.; Xu, Y.; Wang, Z.; Qiu, S.J.; Fan, J.Z. Sorafenib in treatment of patients with advanced hepatocellular carcinoma: A systematic review. *J. Hepatobiliary Pancreat. Dis. Int.* **2012**, *11*, 458–466. [[CrossRef](#)] [[PubMed](#)]
2. Wilhelm, S.M.; Adnane, L.; Newell, P.; Villanueva, A.; Llovet, J.M.; Lynch, M. Preclinical overview of sorafenib, a multikinase inhibitor that targets both Raf and VEGF and PDGF receptor tyrosine kinase signaling. *Mol. Cancer Ther.* **2008**, *7*, 3129–3140. [[CrossRef](#)] [[PubMed](#)]
3. Chen, K.F.; Tai, W.T.; Hsu, C.Y.; Huang, J.W.; Liu, C.Y.; Chen, P.J. Blockade of STAT3 Activation by sorafenib derivatives through enhancing SHP-1 phosphatase activity. *Eur. J. Med. Chem.* **2012**, *55*, 220–227. [[CrossRef](#)] [[PubMed](#)]
4. Tai, W.T.; Cheng, A.L.; Shiau, C.W.; Huang, H.P.; Huang, J.W.; Chen, P.J. Signal transducer and activator of transcription 3 is a major kinase-independent target of sorafenib in hepatocellular carcinoma. *J. Hepatol.* **2011**, *55*, 1041–1048. [[CrossRef](#)] [[PubMed](#)]
5. Tang, K.; Luo, C.; Li, Y.; Lu, C.; Zhou, W.; Huang, H. The study of a novel sorafenib derivative HLC-080 as an antitumor agent. *PLoS ONE* **2014**, *9*, e101889. [[CrossRef](#)]
6. Yang, S.; Zhang, B.; Gong, X.; Wang, T.; Liu, Y.; Zhang, N. In vivo biodistribution, biocompatibility, and efficacy of sorafenib-loaded lipid-based nanosuspensions evaluated experimentally in cancer. *Int. J. Nanomed.* **2016**, *11*, 2329–2343.
7. Patel, K.C.; Bothiraja, A.; Mali, R.; Kamble. Investigation of sorafenib tosylate loaded liposomal dry powder inhaler for the treatment of non-small cell lung cancer. *Part. Sci. Technol.* **2021**, *39*, 990–999. [[CrossRef](#)]
8. Pethe, A.M.; Yadav, K.S. Polymers, responsiveness and cancer therapy. *Artif. Cells Nanomed. Biotechnol.* **2019**, *47*, 395–405. [[CrossRef](#)]
9. Valencia-Lazcano, A.A.; Hassan, D.; Pourmadadi, M.; Shamsabadipour, A.; Behzadmehr, R.; Rahdar, A.; Medina, D.I.; Díez-Pascual, A.M. 5-Fluorouracil nano-delivery systems as a cutting-edge for cancer therapy. *Eur. J. Med. Chem.* **2023**, *246*, 114995. [[CrossRef](#)]
10. Caro, C.; Pourmadadi, M.; Eshaghi, M.M.; Rahmani, E.; Shojaei, S.; Paiva-Santos, A.C.; Rahdar, A.; Behzadmehr, R.; García-Martín, M.L.; Díez-Pascual, A.M. Nanomaterials loaded with quercetin as an advanced tool for cancer treatment. *J. Drug Deliv. Sci. Tech.* **2022**, *78*, 103938. [[CrossRef](#)]
11. Thapa, R.K.; Choi, J.Y.; Poudel, B.K.; Hiep, T.T.; Pathak, S.; Gupta, B. Multilayer-coated liquid crystalline nanoparticles for effective sorafenib delivery to hepatocellular carcinoma. *ACS Appl. Mater. Interfaces* **2015**, *7*, 20360–20368. [[CrossRef](#)] [[PubMed](#)]
12. Chen, J.; Sheu, A.Y.; Li, W.; Zhang, Z.; Kim, D.H.; Lewandowski, R.J. Poly(lactide-co-glycolide) Microspheres for MRI-monitored Transcatheter Delivery of Sorafenib to Liver Tumors. *J. Control Release.* **2014**, *184*, 10–17. [[CrossRef](#)]
13. Kong, F.K.; Ye, Q.F.; Miao, X.Y.; Liu, X.; Huang, S.Q.; Xiong, L.; Yu, W.; Zhang, Z.J. Current status of sorafenib nanoparticle delivery systems in the treatment of hepatocellular carcinoma. *Theranostics* **2021**, *11*, 5464–5490. [[CrossRef](#)]
14. Chen, F.M.; Fang, Y.F.; Chen, X.; Deng, R.; Zhang, Y.J.; Shao, J.W. Recent advances of sorafenib nanoformulations for cancer therapy: Smart nanosystem and combination therapy. *Asian J. Pharm. Sci.* **2021**, *16*, 318–336. [[CrossRef](#)] [[PubMed](#)]
15. Hrushikesh, R.; Chetana, J.; Karishma, S.; Neha, L.; Harsh, P.; Nijhawan, H.P.; Rao, G.K.; Rajasekhar, R.A.; Garima, J.C.; Patro, N.J.; et al. Sorafenib tosylate novel drug delivery systems: Implications of nanotechnology in both approved and unapproved indications. *OpenNano* **2022**, *8*, 100103.
16. Shukla, S.K. Sorafenib loaded inhalable polymeric nanocarriers against non-small cell lung cancer. *Pharm. Res.* **2020**, *37*, 67. [[CrossRef](#)]
17. Angela Gauthier, A.; Ho, M. Role of sorafenib in the treatment of advanced hepatocellular carcinoma: An update. *Hepatol. Res.* **2013**, *43*, 147–154. [[CrossRef](#)]
18. Li, M.; Su, Y.; Zhang, F.G.; Chen, K.R.; Xu, X.T.; Xu, L.; Zhou, J.P.; Wang, W. A dual-targeting reconstituted high density lipoprotein leveraging the synergy of sorafenib and anti-miRNA21 for enhanced hepatocellular carcinoma therapy. *Acta Biomater.* **2018**, *75*, 413–426. [[CrossRef](#)]
19. Muller, R.H.; Runge, S.A.; Ravelli, V.; Thunemann, A.F.; Mehnert, W.; Souto, E.B. Cyclosporine-loaded solid lipid nanoparticles (SLN): Drug-lipid physicochemical interactions and characterization of drug incorporation. *Eur. J. Pharm. Biopharm.* **2008**, *68*, 535–544. [[CrossRef](#)]
20. Menon, I.; Zaroudi, M.; Zhang, Y.; Aisenbrey, E.; Hui, L. Fabrication of active targeting lipid nanoparticles: Challenges and perspectives. *Mater. Today Adv.* **2022**, *16*, 100299. [[CrossRef](#)]
21. Mahmoodi, N.O.; Alavi, S.M.; Yahyazadeh, A. Formulation and therapeutic efficacy of PEG-liposomes of sorafenib for the production of NL-PEG-SOR FUM and NL-PEG-SOR TOS. *Res. Chem. Intermed.* **2022**, *48*, 3915–3935. [[CrossRef](#)]
22. Bondi, M.L.; Botto, C.; Amore, E.; Emma, M.R.; Augello, G.; Craparo, E.F.; Cervello, C. Lipid nanocarriers containing sorafenib inhibit colonies formation in human hepatocarcinoma cells. *Int. J. Pharm.* **2015**, *493*, 75–85. [[CrossRef](#)] [[PubMed](#)]
23. Wang, H.; Wang, H.Y.; Yang, W.L.; Yu, M.J.; Sun, S.L.; Xie, B.G. Improved oral bioavailability and liver targeting of sorafenib solid lipid nanoparticles in rats. *AAPS PharmSciTech.* **2018**, *19*, 761–768. [[CrossRef](#)] [[PubMed](#)]
24. Sebastien, B.; Ferey, L.; Bruno, A.; Mebarek, N.; Gaele, V.; Ananda, A.; Cathy, S.; Karen, G.; Philippe, B. Nucleoside-lipid-based nanocarriers for sorafenib delivery. *Nanoscale Res. Lett.* **2018**, *13*, 17–24.

25. Ahiwale, R.J.; Chellampillai, B.; Pawar, A.P. Investigation of novel sorafenib tosylate loaded biomaterial-based nano-cochleates dispersion system for treatment of hepatocellular carcinoma. *J. Dispers. Sci. Technol.* **2022**, *43*, 1568–1586. [[CrossRef](#)]
26. Bartos, A.; Iancu, I.; Ciobanu, L.; Onaciu, A.; Moldovan, C.; Moldovan, A.; Moldovan, R.C.; Tigu, A.B.; Stiuftuc, G.F.; Toma, V.; et al. Hybrid lipid nanoformulations for hepatoma therapy: Sorafenib loaded nanoliposomes—A preliminary study. *Nanomaterials* **2022**, *12*, 2833. [[CrossRef](#)]
27. Ye, H.; Zhou, L.; Jin, H.; Chen, Y.; Cheng, D.; Jiang, Y. Sorafenib-loaded long-circulating nanoliposomes for liver cancer therapy. *BioMed Res. Inter.* **2020**, *2020*, 1351046. [[CrossRef](#)]
28. Liu, R.; Meng, Y.; Zhu, M.; Zhai, H.; Lv, W.; Wen, T.; Jin, N. Study on novel PtNP–sorafenib and its interaction with VEGFR2. *J. Biochem.* **2021**, *170*, 411–417. [[CrossRef](#)]
29. Yang, Y.C.; Cai, J.; Yin, J.; Zhang, J.; Wang, K.L.; Zhang, Z.T. Heparin-functionalized pluronic nanoparticles to enhance the antitumor efficacy of sorafenib in gastric cancers. *Carbohydr. Polym.* **2016**, *136*, 782–790. [[CrossRef](#)]
30. Jaleh, V.; Fatemeh, R.; Mahboubeh, R.; Ali, J. PEGylated trimethylchitosan emulsomes conjugated to octreotide for targeted delivery of sorafenib to hepatocellular carcinoma cells of HepG2. *J. Liposome Res.* **2019**, *31*, 64–78.
31. Yao, Y.; Su, Z.; Liang, Y.; Zhang, N. pH-Sensitive carboxymethyl chitosan-modified cationic liposomes for sorafenib and siRNA co-delivery. *Int. J. Nanomed.* **2015**, *10*, 6185–6197.
32. Dayani, L.; Dehghani, M.; Aghaei, M.; Taymouri, S.; Taheri, A. Preparation and evaluation of targeted albumin lipid nanoparticles with lactobionic acid for targeted drug delivery of sorafenib in hepatocellular carcinoma. *J. Drug Deliv. Sci. Tech.* **2022**, *69*, 103142. [[CrossRef](#)]
33. Gopakumar, L.; Sreeranganathan, M.; Chappan, S. Enhanced oral bioavailability and antitumor therapeutic efficacy of sorafenib administered in core-shell protein nanoparticle. *Drug Deliv. Transl. Res.* **2022**, *12*, 2824–2837. [[CrossRef](#)] [[PubMed](#)]
34. Loftsson, T.; Brewster, M.E. Pharmaceutical applications of cyclodextrins: Basic science and product development. *J. Pharm. Pharmacol.* **2010**, *62*, 1607–1621. [[CrossRef](#)]
35. Bondi, M.L.; Scala, A.; Sortino, G.; Amore, E.; Botto, C.; Azzolina, A.; Balasus, D.; Cervello, M.; Mazzaglia, A. Nanoassemblies based on supramolecular complexes of nonionic amphiphilic cyclodextrin and sorafenib as effective weapons to kill human HCC cells. *Biomacromolecules* **2015**, *16*, 3784–3791. [[CrossRef](#)]
36. Mo, L.X.; Song, J.G.; Lee, H.K.; Zhao, M.J.; Kim, H.Y.; Lee, Y.J.; Ko, H.W.; Han, H.Y. PEGylated hyaluronic acid-coated liposome for enhanced in vivo efficacy of sorafenib via active tumor cell targeting and prolonged systemic exposure. *Nanomedicine* **2018**, *14*, 557–567. [[CrossRef](#)]
37. Zhang, W.; Cai, J.; Wu, B.; Shen, Z. pH-responsive hyaluronic acid nanoparticles coloaded with sorafenib and cisplatin for treatment of hepatocellular carcinoma. *J. Biomater. Appl.* **2019**, *34*, 219–228. [[CrossRef](#)]
38. Kim, D.H.; Kim, M.D.; Choi, C.W.; Chung, C.W.; Ha, S.H.; Kim, C.H.; Shim, Y.H.; Jeong, Y.; Kang, D.H. Antitumor activity of sorafenib-incorporated nanoparticles of dextran/poly(dl-lactide-co-glycolide) block copolymer. *Nanoscale. Res Lett.* **2012**, *7*, 91. [[CrossRef](#)]
39. Lin, T.T.; Gao, D.Y.; Liu, Y.C.; Sung, Y.C.; Wan, D.H.; Liu, J.Y.; Chiang, T.; Wang, L.Y.; Chen, Y.C. Development and characterization of sorafenib-loaded PLGA nanoparticles for the systemic treatment of liver fibrosis. *J. Control. Release* **2016**, *221*, 62–70. [[CrossRef](#)]
40. Monajati, M.; Tavakoli, S.; Abolmaali, S.S.; Yousefi, G.; Tamaddon, A. Effect of PEGylation on assembly morphology and cellular uptake of poly ethyleneimine-cholesterol conjugates for delivery of sorafenib tosylate in hepatocellular carcinoma. *BioImpacts* **2018**, *8*, 1–252. [[CrossRef](#)]
41. Melchiorre, C.; Giovanna, P.; Antonella, B.V.; Barbara, P.; Daniele, B.; Maria, R.E.; Antonina, A.; Roberto, P.; Guido, R.L.; Stefano, P.; et al. Nanoparticles of a polyaspartamide-based brush copolymer for modified release of sorafenib: In vitro and in vivo evaluation. *J. Control. Release* **2017**, *266*, 47–56.
42. Yang, D.; Armitage, B.; Marder, S.R. Cubic Liquid-crystalline nanoparticles. *Angew. Chem. Int. Ed.* **2004**, *43*, 4402–4409. [[CrossRef](#)] [[PubMed](#)]
43. Liu, Y.; Yang, J.; Wang, X.; Liu, J.; Wang, Z.; Liu, H. In vitro and in vivo evaluation of redox-responsive sorafenib carrier nanomicelles synthesized from poly(acrylic acid)-cystamine hydrochloride-D-alpha-tocopherol succinate. *J. Biomater. Sci. Polym. Ed.* **2016**, *27*, 1729–1747. [[CrossRef](#)]
44. Känkänen, V.; Fernandes, M.; Liu, Z.; Seitsonen, J.; Hirvonen, S.; Ruokolainen, J.; Pinto, J.F.; Hirvonen, J.; Balasubramanian, V.; Santos, H.A. Microfluidic preparation and optimization of sorafenib-loaded poly(ethylene glycol-block-caprolactone) nanoparticles for cancer therapy applications. *J. Colloid Interface Sci.* **2023**, *633*, 383–395. [[CrossRef](#)] [[PubMed](#)]
45. Shi, L.; Hu, Y.; Lin, A.; Ma, C.; Zhang, C.; Su, Y. Matrix metalloproteinase responsive nanoparticles for synergistic treatment of colorectal cancer via simultaneous anti-angiogenesis and chemotherapy. *Bioconjug. Chem.* **2016**, *27*, 2943–2953. [[CrossRef](#)]
46. Fan, W.; Shen, B.; Bu, W.; Chen, F.; He, Q.; Zhao, K.; Zhang, S.; Zhou, L.; Xiao, Q.; Ni, D.; et al. A smart upconversion-based mesoporous silica nanotheranostic system for synergetic chemo-/radio-/photodynamic therapy and simultaneous MR/UCL imaging. *Biomaterials* **2014**, *35*, 8992–9002. [[CrossRef](#)]
47. Barkat, A.; Beg, S.; Panda, S.K.; Alharbi, S.K.; Rahman, M.; Ahmed, F.J. Functionalized mesoporous silica nanoparticles in anticancer therapeutics. *Semin Cancer Biol.* **2021**, *69*, 365–375. [[CrossRef](#)]
48. Zheng, G.; Zhao, R.; Xu, A.; Shen, Z.; Chen, X.; Shao, J. Co-delivery of sorafenib and siVEGF based on mesoporous silica nanoparticles for ASGPR mediated targeted HCC therapy. *Eur. J. Pharmac. Sci.* **2018**, *111*, 492–502. [[CrossRef](#)]

49. Zhang, B.C.; Luo, B.Y.; Zou, J.J.; Wu, P.Y.; Jiang, J.L.; Le, J.L.; Zhao, R.R.; Chen, L.; Shao, J.W. Co-delivery of sorafenib and CRISPR/Cas9 based on targeted core-shell hollow mesoporous organosilica nanoparticles for synergistic HCC therapy. *ACS Appl. Mater. Interfaces*. **2020**, *12*, 57362–57372. [[CrossRef](#)]
50. Tang, H.; Chen, D.; Li, C.; Zheng, C.; Wu, X.; Zhang, Y. Dual GSH-exhausting sorafenib loaded manganese-silica nanodrugs for inducing the ferroptosis of hepatocellular carcinoma cells. *Int. J. Pharm.* **2019**, *572*, 118782. [[CrossRef](#)]
51. Li, B.; Zhang, X.; Wu, Z.; Chu, T.; Yang, Z.; Xu, S.; Wu, S.; Qie, Y.; Lu, Z.; Qi, F.; et al. Reducing postoperative recurrence of early-stage hepatocellular carcinoma by a wound-targeted nanodrug. *Adv. Sci.* **2022**, *9*, 2200477. [[CrossRef](#)]
52. Dave, V.; Sharma, R.; Gupta, C.; Sur, C. Folic acid modified gold nanoparticle for targeted delivery of Sorafenib tosylate towards the treatment of diabetic retinopathy. *Colloids Surf. B Biointerfaces* **2020**, *194*, 111151. [[CrossRef](#)]
53. Cai, H.; Yang, Y.; Peng, Y.; Liu, Y.; Fu, X.; Ji, B. Gold nanoparticles-loaded anti-mir221 enhances antitumor effect of sorafenib in hepatocellular carcinoma cells. *Int. J. Med. Sci.* **2019**, *16*, 1541–1548. [[CrossRef](#)] [[PubMed](#)]
54. Sukkar, F.; Shafaa, M.; Nagdy, M.; Darwish, W.; Korraa, S. Alginate/CaCO₃ hybrid loaded with sorafenib tosylate and gold hexagons: A model for efficient dual (Chemo-Radio) treatment of HepG2 cells. *Egypt. J. Chem.* **2021**, *16*, 8309–8321. [[CrossRef](#)]
55. Moni, S.S.; Alam, M.F.; Safhi, M.M.; Sultan, M.H.; Makeen, H.A.; Elmobark, M.E. Development of formulation methods and physical characterization of injectable sodium selenite nanoparticles for the delivery of sorafenib tosylate. *Curr. Pharm. Biotechnol.* **2020**, *21*, 659–666. [[CrossRef](#)]
56. Zheng, L.; Li, C.; Huang, X.; Lin, X.; Lin, W.; Yang, F.; Chen, T. Thermosensitive hydrogels for sustained release of sorafenib and selenium nanoparticles for localized synergistic chemoradiotherapy. *Biomaterials* **2019**, *216*, 119220. [[CrossRef](#)] [[PubMed](#)]
57. Jin, S.E.; Jin, H.E. Synthesis, characterization, and three-dimensional structure generation of zinc oxide-based nanomedicine for biomedical applications. *Pharmaceutics* **2019**, *11*, 575. [[CrossRef](#)]
58. Nabil, A. Zinc oxide nanoparticle synergizes sorafenib anticancer efficacy with minimizing its cytotoxicity. *Oxid. Med. Cell. Longev.* **2020**, *2020*, 1362104. [[CrossRef](#)]
59. György, B.; Biró, E.; Mónika, M.; Tivadar, F. Dual drug delivery of sorafenib and doxorubicin from PLGA and PEG-PLGA polymeric nanoparticles. *Polymers* **2018**, *10*, 895.
60. Duan, D.W.; Liu, Y. Targeted and synergistic therapy for hepatocellular carcinoma: Monosaccharide modified lipid nanoparticles for the co-delivery of doxorubicin and sorafenib. *Drug Des. Devel. Ther.* **2018**, *12*, 2149–2161. [[CrossRef](#)]
61. Mato, E.; Puras, G.; Bell, O.; Agirre, M.; Hernández, R.M.; Igartua, M.; Moreno, R.; Gonzalez, G.; Leiva, A.; Pedraz, J.L. Selective antitumoral effect of sorafenib loaded PLGA nanoparticles conjugated with cetuximab on undifferentiated/anaplastic thyroid carcinoma cells. *J. Nanomed. Nanotechnol.* **2015**, *6*, 1000281.
62. Li, S.; Dong, S.; Xu, W.; Jiang, Y.; Li, Z. Polymer nanoformulation of sorafenib and all-trans retinoic acid for synergistic inhibition of thyroid cancer. *Front. Pharmacol.* **2020**, *10*, 1676. [[CrossRef](#)] [[PubMed](#)]
63. Wang, Y.L.; Yu, H.Y.; Zhang, D.W.; Wang, G.Y.; Song, W.T.; Liu, Y.M.; Ma, S.; Tang, Z.H.; Liu, Z.L.; Sakurai, K.; et al. Co-administration of combretastatin A4 nanoparticles and sorafenib before systemic therapy of hepatocellular carcinoma. *Acta Biomater.* **2019**, *92*, 229–240. [[CrossRef](#)] [[PubMed](#)]
64. Bhattacharya, S.; Pawde, D.; Dumpala, R.L. Preparation of Sorafenib tosylate self-emulsified drug delivery system and the effect on combination therapy with Bosutinib against HCT116/SW1417 cells. *Results Chem.* **2022**, *4*, 100385. [[CrossRef](#)]
65. Yin, X.; Xiao, Y.; Han, L.; Zhang, B.; Wang, T.; Su, Z.; Zhang, N. Ceramide-fabricated co-loaded liposomes for the synergistic treatment of hepatocellular carcinoma. *AAPS PharmSciTech.* **2018**, *19*, 2133–2143. [[CrossRef](#)]
66. Sukkar, F.; Shafaa, M.; El-Nagdy, M.; Darwish, W. Polymeric nanocarriers for effective synergistic action of sorafenib tosylate and gold-sensitized gamma radiation against HepG2 Cells. *Inter. J. Nanomed.* **2021**, *16*, 8309–8321. [[CrossRef](#)]
67. Laurent, S.; Saei, A.A.; Behzadi, S.; Panahifar, A.; Mahmoudi, M. Superparamagnetic iron oxide nanoparticles for delivery of therapeutic agents: Opportunities and challenges. *Expert Opin. Drug Deliv.* **2014**, *11*, 1449–1470. [[CrossRef](#)]
68. Rao, Y.F.; Chen, W.; Liang, X.G.; Huang, Y.Z.; Miao, J.; Liu, Y.; Lou, Y.; Zhang, X.G.; Wang, B.; Tang, R.K. Epirubicin-loaded superparamagnetic iron-oxide nanoparticles for transdermal delivery: Cancer therapy by circumventing the skin barrier. *Small* **2015**, *11*, 239–247. [[CrossRef](#)]
69. Taratula, O.; Garbuzenko, O.; Savla, R.; Wang, Y.A.; Minko, H.T. Multifunctional nanomedicine platform for cancer-specific delivery of siRNA by superparamagnetic iron oxide nanoparticles-dendrimer complexes. *Curr. Drug Deliv.* **2011**, *8*, 59–69. [[CrossRef](#)]
70. Grillone, A.; Riva, E.R.; Mondini, A.; Forte, C.; Calucci, L.; Innocenti, C.; de Julian Fernandez, C.; Cappello, V.; Gemmi, M.; Moscato, S.; et al. Active targeting of sorafenib: Preparation, characterization, and in vitro testing of drug-loaded magnetic solid lipid nanoparticles. *Adv. Healthc. Mater.* **2015**, *4*, 1681–1690. [[CrossRef](#)]
71. Greeshma, T.; Sheena, P.; Rimal, I.; Praseetha, P.K.; Jiji, S.G.; Asha, V.V. Preparation of an efficient and safe polymeric-magnetic nanoparticle delivery system for sorafenib in hepatocellular carcinoma. *Life Sci.* **2018**, *206*, 10–21.
72. Cai, M.; Li, B.; Lin, L.; Huang, J.; An, Y.; Huang, W.; Zhou, Z.; Wang, Y.; Shuai, X.; Zhu, K. A reduction and pH dual-sensitive nanodrug for targeted theranostics in hepatocellular carcinoma. *Biomater. Sci.* **2020**, *8*, 3485–3499. [[CrossRef](#)]
73. Amir, H.; Homayon, A.P.; Mehdi, F.; Fatemeh, F. Synthesis of thermosensitive magnetic nanocarrier for controlled sorafenib delivery. *Mater. Sci. Eng. C.* **2016**, *67*, 42–50.

74. Dahiya, M.; Awasthi, R.; Dua, K.; Dureja, H. Sorafenib tosylate loaded superparamagnetic nanoparticles: Development, optimization and cytotoxicity analysis on HepG2 human hepatocellular carcinoma cell line. *J. Drug Deliv. Sci. Tech.* **2023**, *79*, 104044. [[CrossRef](#)]
75. Xiao, Y.; Liu, Y.J.; Yang, S.; Zhang, B.; Wang, T.Q.; Jiang, D.D.; Zhang, J.; Yu, D.X.; Zhang, N. Sorafenib and gadolinium co-loaded liposomes for drug delivery and MRI-guided HCC treatment. *Colloids Surf. B.* **2016**, *141*, 83–92. [[CrossRef](#)] [[PubMed](#)]
76. Xu, W.; Qing, X.; Liu, S.; Yang, D.; Dong, X.; Zhang, Y. Hollow mesoporous manganese oxides: Application in cancer diagnosis and therapy. *Small* **2022**, *18*, e2106511. [[CrossRef](#)] [[PubMed](#)]
77. Xu, X.; Duan, J.; Liu, Y.; Kuang, Y.; Duan, Y.; Liao, J.; Xu, T.; Jiang, Z.; Li, B. Multi-stimuli responsive hollow MnO₂-based drug delivery system for magnetic resonance imaging and combined chemo-chemodynamic cancer therapy. *Acta Biomater.* **2021**, *126*, 445–462. [[CrossRef](#)]
78. Wang, Z.; Wu, C.; Liu, J.; Hu, S.; Yu, J.; Yin, Q.; Tian, H.; Ding, Z.; Qi, G.; Wang, L.; et al. Aptamer-mediated hollow MnO₂ for targeting the delivery of sorafenib. *Drug Deliv.* **2023**, *30*, 28–39. [[CrossRef](#)]
79. Xu, X.; Chen, Y.; Gui, J.; Liu, P.; Huang, Y.; Shao, B.; Ping, Y.; Li, B. A biomimetic nanodrug self-assembled from small molecules for enhanced ferroptosis therapy. *Biomater. Sci.* **2022**, *10*, 770–780. [[CrossRef](#)]
80. Liu, Y.; Xu, M.; Dai, Y.; Zhao, Q.; Zhu, L.; Guan, X.; Li, G.; Yang, S.; Yuan, Z. NIR-II dual-modal optical coherence tomography and photoacoustic imaging-guided dose-control cancer chemotherapy. *ACS Appl. Polym. Mater.* **2020**, *2*, 1964–1973. [[CrossRef](#)]
81. Park, J.Y.; You, S.J.; Park, K.; Song, Y.J.; Park, J.; Yang, D.H. Cyclic RGDfK- and Sulfo-Cy5.5-functionalized mPEG-PCL theranostic nanosystems for hepatocellular carcinoma. *J. Indus. Eng. Chem.* **2021**, *99*, 204–213. [[CrossRef](#)]
82. Feng, S.; Zhou, J.; Li, Z.; Appelman, H.D.; Zhao, L.L.; Zhu, J.Y.; Thomas, D. Sorafenib encapsulated in nanocarrier functionalized with glypican-3 specific peptide for targeted therapy of hepatocellular carcinoma. *Colloids Surf. B.* **2019**, *184*, 10. [[CrossRef](#)] [[PubMed](#)]
83. Lakshmi, T.K.; Hitesh, K.; Lakshma, N.V.; Madhusudana, M.; Suresh, B.; Deep, P.; Ramakrishna, S. Modulating the site-specific oral delivery of sorafenib using sugar-grafted nanoparticles for hepatocellular carcinoma treatment. *Eur. J. Pharm. Sci.* **2019**, *137*, 104978.
84. Li, Y.W.; Wei, J.J.; Wei, Y.H.; Cheng, L.; Guo, B.B.; Meng, F.H.; Li, F.; Zhong, Z.Y. Apolipoprotein E peptide-guided disulfide-cross-linked micelles for targeted delivery of sorafenib to hepatocellular carcinoma. *Biomacromolecules* **2020**, *21*, 716–724. [[CrossRef](#)]
85. Gao, D.Y.; Lin, T.T.; Sung, Y.C.; Liu, Y.C.; Chiang, W.H.; Chang, C.H.; Liu, J.Y.; Chen, Y.C. CXCR4-targeted lipid-coated PLGA nanoparticles deliver sorafenib and overcome acquired drug resistance in liver cancer. *Biomaterials* **2015**, *67*, 194–203. [[CrossRef](#)]
86. Zhang, L.; Gong, F.; Zhang, F. Targeted therapy for humanhepatic carcinoma cells using folate-functionalized polymeric micelles loaded with superparamagnetic iron oxide and sorafenib in vitro. *Int. J. Nanomed.* **2013**, *8*, 1517–1524. [[CrossRef](#)]
87. Li, Y.J.; Dong, M.; Kong, F.M. Folate-decorated anticancer drug and magnetic nanoparticles encapsulated polymeric carrier for liver cancer therapeutics. *Int. J. Pharm.* **2015**, *489*, 83–90. [[CrossRef](#)]
88. Wang, H.P.; Sun, S.L.; Zhang, Y.; Wang, J.Y.; Zhang, S.H.; Yao, X.B.; Chen, L.; Gao, Z.; Xie, B.G. Improved drug targeting to liver tumor by sorafenib-loaded folate-decorated bovine serum albumin nanoparticles. *Drug Deliv.* **2019**, *26*, 89–97. [[CrossRef](#)]
89. Meng, T.; Li, Y.; Tian, Y.; Ma, M.; Shi, K.; Shang, X.; Yuan, H.; Hu, F. A Hypoxia-sensitive drug delivery system constructed by nitroimidazole and its application in the treatment of hepatocellular carcinoma. *AAPS PharmSciTech.* **2022**, *23*, 167. [[CrossRef](#)]
90. Shen, J.; Cai, W.; Ma, Y.; Xu, R.; Huo, Z.; Song, L. hGC33-Modified and sorafenib-loaded nanoparticles have a synergistic anti-hepatoma effect by inhibiting Wnt signaling pathway. *Nanoscale Res. Lett.* **2020**, *15*, 220. [[CrossRef](#)]
91. Lin, J.; Zhang, J.; Wang, K.; Guo, S.; Yang, W. Zwitterionic polymer coated sorafenib-loaded Fe₃O₄ composite nanoparticles induced ferroptosis for cancer therapy. *J. Mater. Chem. B* **2022**, *10*, 5784–5795. [[CrossRef](#)] [[PubMed](#)]
92. Zhou, K.; Xu, W.; Zhang, X.; Wang, S.; Li, Y.; Yang, L.; Cai, R.; Xu, Q.; Li, G.; Guo, X. Complex of nanocarriers based on the metal polyphenol network: Multi-modal synergistic inhibition of tumor cell proliferation by inducing ferroptosis and photodynamic effect. *New J. Chem.* **2022**, *46*, 21962–21967. [[CrossRef](#)]
93. Han, L.; Liang, S.; Mu, W.; Zhang, Z.; Wang, L.; Ouyang, S.; Yao, B.; Liu, Y.; Zhang, N. Amphiphilic small molecular mates match hydrophobic drugs to form nanoassemblies based on drug-mate strategy. *Asian J. Pharm. Sci.* **2022**, *17*, 129–138. [[CrossRef](#)] [[PubMed](#)]

Disclaimer/Publisher’s Note: The statements, opinions and data contained in all publications are solely those of the individual author(s) and contributor(s) and not of MDPI and/or the editor(s). MDPI and/or the editor(s) disclaim responsibility for any injury to people or property resulting from any ideas, methods, instructions or products referred to in the content.